Numerical Analysis of Core Melt Solidification and Spreading Behavior Using the MPS Method

Yun Sik Cho [1], JinHo Song [1,] Sung Joong Kim [1,2] *
[1] Department of Nuclear Engineering, Hanyang University
[2] Institute of Nano Science & Technology, Hanyang University
222 Wangsimni-ro, Seongdong-gu, Seoul, 04763, Republic of Korea
yunscho@hanyang.ac.kr; chsong@hanyang.ac.kr; sungjkim@hanyang.ac.kr*

***Keywords : MPS, Lagrangian, CFD, Melt Spreading, Solidification**

1. Introduction

After the Three Mile Island (TMI) and Fukushima accidents, the need for comprehensive safety analysis of severe accidents has become a major focus in nuclear research. In postulated severe accident scenarios, such as the failure of emergency core cooling systems, molten corium can be generated and released from the reactor pressure vessel (RPV), significantly influencing accident progression. Among these phenomena, molten corium spreading and solidification behavior are key factors in determining accident consequences. Particularly, the formation of a crust layer at the surface of the molten corium can impact heat transfer and flow dynamics, making accurate prediction of solidification behavior essential for severe accident assessment. Previous studies have investigated molten corium behavior and solidification through both experimental research and computational analysis, including empirical correlations.

Many studies simulate behavior of molten corium by pouring molten corium into stainless-steel substrate. KATS [1] and SPREAD [2] was one of the representative spreading test facility using oxide simulant. While the interpretation of heat removal and solidification by radiative heat transfer was sufficiently observable, the phase change tendency which include re-melting and substrate ablation, cannot be simulated due to limit of similarity experiment, which is difference in thermal properties including heat capacity, thermal conductivity, and melting point. Experimental study using reactor material also be conducted by Magallon and Tromm [3] using FARO facility and Cognet et al and Journeau et al [4-6] using VULCANO facility. FARO [3] test which conducted two kind of corium test on dry surface and wet surface of steel substrate, measure time-dependent spreading behavior of mixture of molten uranium and zirconium oxide. On the other hand, the test from VULCANO [4-6] facility measured not only spreading behavior but also temperature distribution of molten corium consisting of uranium, zirconium oxide, iron, and ceramics on both ceramic and iron substrate.

However, As the test material was not activated unlike reactor material, experimental studies still have limit that the effect of decay heat and chemical reaction, which is a major property of Corium causing re-melting, still cannot be considered.

Prediction using numerical analysis of the melt spread process has also been conducted to overcome the limit of the above experiments. For example, Eulerian-based Lumped parameter codes, MELT SPREAD [7], THEMA [8-9] and CORFLOW [10] were developed to simulate analysis for severe accident and mitigation strategy. MELTSPREAD code was developed to simulate spreading while accounting for the effects of heat transfer and phase change including solidification and ablation. The MELTSPREAD [7] calculate locally averaged conservation equation with one-dimensional computing domain. The same approach is used in THEMA [8-9] and CORFLOW [10], but each codes expanded the calculation domain from one-dimension to two-dimension and three-dimension approach, respectively. However, since the Eulerian numerical analysis, which relies on the above empirical formula and computational domain, it is more appropriate for Corium analysis to use Lagrangian approaches which are suitable for interpretation of changes in phase and thermal property of simulated particles and changes in computational domain. Lagrangian-based simulation also be conducted mainly through Moving Particle Semi-implicit (MPS) which shows high accuracy in fluid dynamics, heat transfer, and phase change of incompressible fluids for Corium analysis. The previous study [11] about corium analysis using MPS method has been sufficiently achieved, while interpretations still show a little high error rate caused by assumptions for simplification of calculation such as discretely divided viscosity range in liquid phase or leaving out property change in phase transition.

The objective of this study is to develop an enhanced MPS-based computational framework incorporating an advanced phase-change model and evaluate its applicability to next-generation reactors. To achieve this, a physics-based numerical approach is implemented in MPS to improve heat transfer and phase change modeling without reliance on empirical correlations. This study develops two object-oriented programming (OOP) modules; Phase-Change Enhanced MPS

Framework and Applicability Assessment for Next-Generation Reactors.

To verify and validate the proposed MPS framework, the results are compared with previous numerical models and experimental data related to melt spreading and solidification. This research aims to establish an accurate, physics-based computational framework applicable to severe accident scenarios in next-generation nuclear reactors.

2. Numerical Method

2.1. Governing Equation for MMPS Method

MPS is one of the Lagrangian-based computational fluid dynamics (CFD) methods which means particle - tracking simulation methods developed to analyze incompressible fluid such as water or metals. The MPS calculation is conducted through tracking variables of particles such as the coordinates, speed, pressure, and temperature. As shown in Figure 1, the MPS calculates fluid dynamics using the interaction with neighboring particles existing within effective radius which is a certain distance radius from the calculating particles. For this purpose, Kernel function in equation (1) was used and it quantifies the degree of interaction over distance. without generating a computational grid, Lagrangian-based CFD employ numerical models using partial differential operators such as gradient, divergence and laplacian operators with Kernel function.

$$w(r) = \begin{cases} \frac{r_e}{r_{ij}} - 1 & (0 < r_{ij} \le r_e) \\ 0 & (r_e \le r_{ij}) \end{cases} \quad (1)$$

2.1.1. Multi-phase Flow analysis model

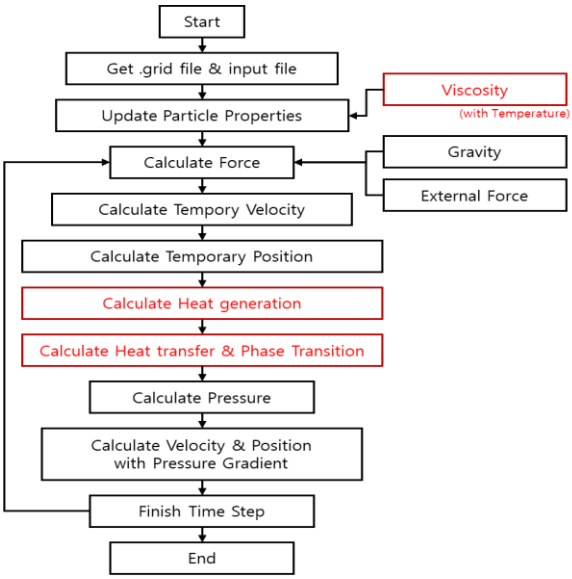

Fig. 1. Algorithm for MPS calculation.

The Moving Particle Semi-implicit (MPS) method is a Lagrangian-based computational fluid dynamics (CFD) approach designed to model incompressible fluids without a computational grid. Unlike Eulerian methods, MPS tracks discrete particles and their interactions within a defined effective radius, making it particularly suitable for severe accident scenarios, such as molten salt spills in MSRs and core melt progression in PWRs. These phenomena involve complex multiphase interactions, free-surface flows, and phase changes, all of which MPS can effectively capture.

$$\frac{\partial n}{\partial t} + \nabla \cdot (nu) = 0 \quad (2)$$

MPS is governed by mass, momentum, and energy conservation equations. The continuity equation ensures mass conservation:

$$\frac{Du}{Dt} = -\frac{1}{\rho}\nabla P + v\nabla^2 u + F_e \quad (3)$$

Figure 1. Algorithm for MPS calculation.

As mentioned earlier, the MPS method uses kernel function to represent partial differential operators to compute interactions with neighboring particles. Equations (5), (6) and (7) represent the gradient, divergence and Laplacian operators using Kernel function used in the MPS method, respectively.

$$\langle \nabla \phi \rangle_i = \frac{d}{n^0} \sum_{j \ne i} \left[\frac{\phi_j - \phi_i}{|r_j - r_i|^2} (r_j - r_i) w(|r_j - r_i|) \right] \quad (4)$$

$$\langle \nabla \cdot \phi \rangle_i = \frac{d}{n^0} \sum_{j \ne i} \frac{(\phi_j - \phi_i) \cdot (r_j - r_i)}{|r_j - r_i|^2} w(|r_j - r_i|) \quad (5)$$

$$\langle \nabla^2 \phi \rangle_i = \frac{2d}{n^0 \lambda} \sum_{j \ne i} (\phi_j - \phi_i) w(|r_j - r_i|) \quad (6)$$

$$\lambda = \frac{\int_V w(r) r^2 dv}{\int_V w(r)\, dv} \quad (7)$$

As shown in equation (9), the explicit step computes the velocity vector of the temporary step using terms of convection and external force in the right-hand side of equation (3).

$$u^* = u^t + \Delta t \left[\frac{2dv_{ij}}{n^0 \lambda} \sum_{j \ne i} (u_j - u_i) w(|r_j - r_i|) + F_e \right] \quad (8)$$

$$\nu_{ij} = \frac{2\nu_i\nu_j}{\nu_i + \nu_j} \quad (9)$$

In the implicit step, the Laplacian pressure term is calculated using the pressure gradient:

$$\nabla^2 P^{n+1} = \frac{\rho}{\Delta t}\langle \nabla \cdot u^* \rangle_i \quad (10)$$

Pressure is solved implicitly using a Poisson equation, stabilizing simulations in multiphase environments:

$$\nabla^2 P^{n+1} = \frac{\rho}{(\Delta t)^2}\frac{n^* - n^0}{n^0} \quad (11)$$

For numerical stability, a multi-source term model is employed by combining both equations:

$$\langle \nabla^2 P \rangle_i = \frac{2d}{n^0\lambda}\sum_{j\neq i}(P_j - P_i)w(|r_j - r_i|) = \alpha_1\frac{\rho}{\Delta t}\langle \nabla \cdot u^* \rangle_i + \alpha_2\frac{\rho}{(\Delta t)^2}\frac{n^* - n^0}{n^0} \quad (12)$$

where α_1 and α_2 are weighting factors, set to 0.8 and 0.2, respectively. These equations form the basis for fluid flow simulation using the MPS method.

Velocity correction is then performed as:

$$u^{t+\Delta t} - u^* = -\frac{\Delta t}{\rho}\nabla P^{t+\Delta t} \quad (11)$$

Where ρ_{ij} is the mean density used for multiphase interactions:

$$\rho_{ij} = \begin{cases} \frac{\rho_i + \rho_j}{2} & j\,particle \neq wall \\ \rho_i & j\,particle = wall \end{cases} \quad (14)$$

This equation ensures that the velocity update is performed consistently across the multiphase system by utilizing the arithmetic mean of the densities of interacting particles. By incorporating density-weighted averaging, the implicit pressure-based correction prevents numerical instabilities and guarantees smooth particle interactions in multiphase simulations.

The corrected velocity is then used to update the position of each particle, ensuring that fluid motion follows physical conservation laws while accurately capturing the interaction between molten salt and its surrounding environment. The next section further explores the role of boundary conditions in defining interaction constraints and enforcing realistic flow behavior.

2.1.2. Heat transfer and Phase Change model

In severe accident analysis, heat transfer and phase transitions play a crucial role in modeling molten materials. The energy conservation equation governs heat transport:

$$\frac{\partial H}{\partial t} = \frac{k}{\rho C_p}\nabla^2 H + q''' \quad (15)$$

Where v is the enthalpy, k is the thermal conductivity, ρ is the fluid density, $C_p$is the specific heat capacity, and q''' represents the internal heat generation per unit volume.

$$H^* = H^t + \Delta t\left[\frac{2k_{ij}d}{\rho C_p n^0\lambda}\sum_{j\neq i}(H_j - H_i)w(|r_j - r_i|) + q'''\right] \quad (16)$$

Where k_{ij} is the harmonic mean used for multiphase interactions:

$$k_{ij} = \frac{2k_i k_j}{k_i + k_j} \quad (17)$$

Phase change is incorporated through an enthalpy formulation, where solid, liquid, and mixed-phase states are defined as:

$$T = \begin{cases} T_m + \frac{(H - H_s)}{\rho C_p} & (H < H_s) \\ T_m & (H_s < H < H_l) \\ T_m + \frac{(H - H_l)}{\rho C_p} & (H_l < H) \end{cases} \quad (18)$$

where T_m is the melting temperature, H_s and H_l are the enthalpy values are at the solid and liquid phase boundaries, respectively.

Viscosity is temperature-dependent and follows an exponential relation:

$$\mu(T) = \begin{cases} \mu_s & (T \leq T_m) \\ \mu_i \exp\left(A_i\frac{T_i - T}{T_i T}\right) & (T_i < T < T_{i+1}) \end{cases} \quad (19)$$

For open-boundary simulations such as molten salt leaks or core melts, heat dissipation is modeled using radiative heat transfer:

$$Q = \varepsilon\sigma A T_i^4 \quad (20)$$

(21) $$A = 6\left(1 - \frac{n_i}{n_0}\right) l_0^2$$

Where ε is the emissivity, σ is the Stefan-Boltzmann constant, and A is the effective surface area of the free surface particle, given as:

2.2. Boundary Condition

2.2.1. Free Surface Treatment and Surface Treatment

Boundary conditions play a crucial role in ensuring physical accuracy in multiphase simulations, particularly in molten salt spills or core melt progression.

Free surfaces are detected based on particle number density:

(22) $$n_i < \beta n_0$$

where β is typically set to 0.95 to distinguish fluid from free-surface particles.

Surface tension is implemented using the continuum surface force (CSF) model:

(23) $$F_s = -\sigma\kappa\nabla C$$

Where σ is the surface tension coefficient, κ is the curvature of the interface, and ∇C is the gradient of an artificially defined color function.

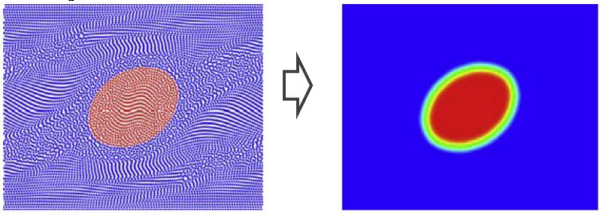

Fig. 2. Schematics of contoured continuum surface force

To improve interface stability, curvature is calculated using the contoured continuum surface force (CCSF) model, which provides robust phase boundary tracking. This method ensures accurate droplet formation, spreading, and solidification, which are essential for molten salt leakage or core melt interactions with structural materials.

3. Result

To evaluate the applicability of the developed MPS-based framework, numerical results were compared with experimental data from KTH experiments and simulation results from KTH MPS, a previous MPS-based study. The comparison focused on leading-edge progression over time, which serves as a key indicator of melt spreading behavior.

As shown in Figure X, the leading-edge predictions from ATHENA MPS (present study) exhibit a similar trend to KTH MPS, demonstrating the capability of the developed model in capturing the overall melt spreading behavior. However, discrepancies are observed in the latter phase of spreading, where ATHENA MPS results tend to underestimate the leading-edge position compared to both the KTH experiment and KTH MPS results.

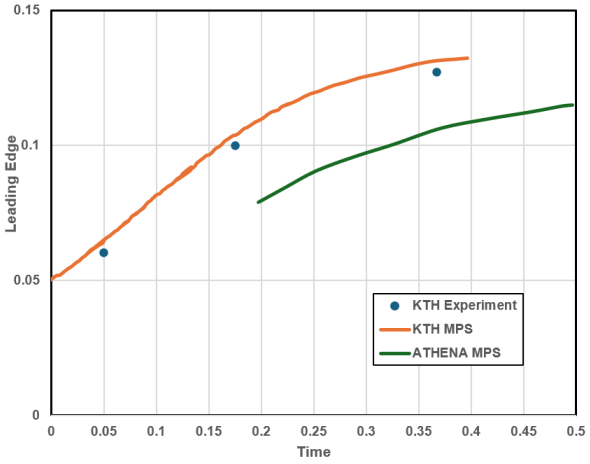

Fig. 3. Comparative Result with KTH

The deviation in ATHENA MPS predictions can be attributed to limitations in viscosity modeling during the phase transition. In the current approach, viscosity is discretized in a stepwise manner, which may introduce inaccuracies in predicting the flow resistance during spreading. Additionally, temperature-dependent variations in viscosity have not been fully accounted for, affecting the heat transfer and phase-change calculations. These aspects contribute to the slower progression of the leading edge in ATHENA MPS compared to KTH MPS and experimental results.

Despite these limitations, the proposed MPS framework successfully captures key melt spreading characteristics and provides a physics-based numerical model for further development.

Further improvements will focus on refining viscosity modeling during phase transition, incorporating a more continuous and temperature-dependent viscosity function to enhance accuracy. Additionally, advanced heat transfer models, including improved treatment of radiative and convective heat loss, will be implemented to minimize discrepancies observed in the latter phase of spreading. These enhancements will contribute to more accurate and predictive simulations for severe accident analysis, particularly for next-generation reactor applications.

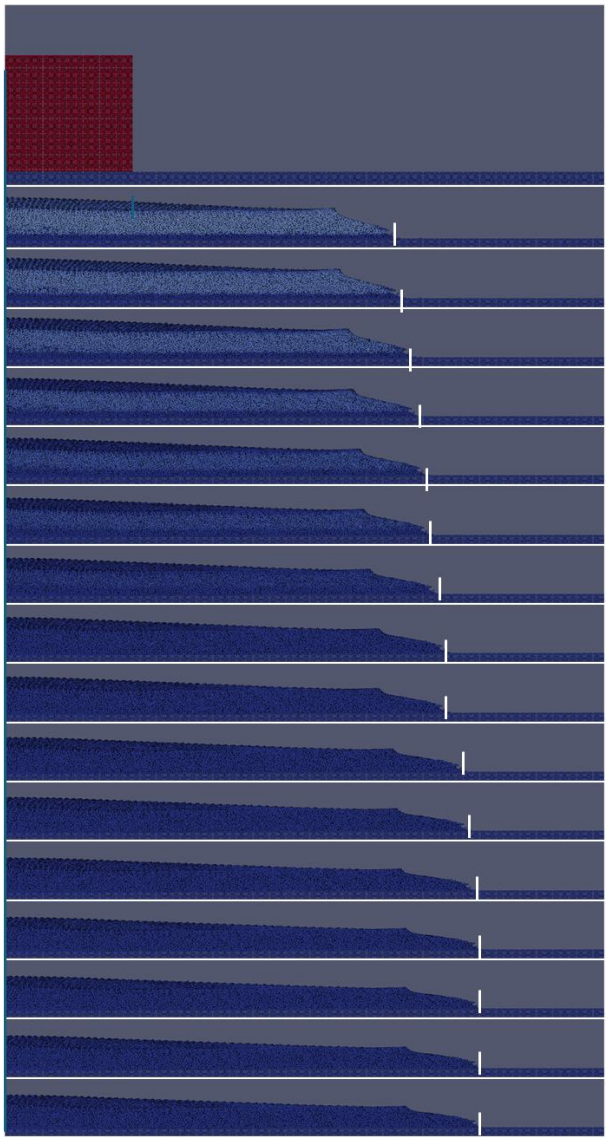

Fig. 4. Images of KTH example using MPS

4. Conclusion

In this study, an MPS-based computational framework incorporating an advanced phase-change model was developed and applied to simulate molten corium spreading and solidification behavior. The objective was to establish a physics-based approach that enhances the predictive capability of the MPS method for severe accident analysis in next-generation nuclear reactors.

The developed ATHENA MPS framework was validated against experimental data from KTH experiments and numerical results from KTH MPS. The comparison of leading-edge progression demonstrated that the proposed model successfully captures the general trend of melt spreading behavior. However, discrepancies were observed in the latter phase of spreading, where ATHENA MPS predictions tended to underestimate the leading-edge position compared to both the experimental data and KTH MPS results. This deviation was attributed to limitations in viscosity modeling during phase transitions, particularly the use of a stepwise viscosity approximation and the lack of a fully temperature-dependent viscosity function.

Despite these limitations, the proposed MPS framework provides a robust numerical foundation for analyzing core melt behavior, solidification, and heat transfer dynamics. To further improve accuracy, future work will focus on refining viscosity modeling, implementing a continuous, temperature-dependent viscosity function, and enhancing the heat transfer model to better capture radiative and convective effects. These improvements will contribute to a more accurate and predictive simulation tool for severe accident scenarios, supporting the application of the MPS method in next-generation reactor safety assessments.

5. Acknowledgments

This research was supported by the National Research Foundation of Korea (NRF) and funded by the ministry of Science, ICT, and Future Planning, Republic of Korea (grant numbers NRF-2021M2D2A2076382) and This work was supported by the Human Resources Development of the Korea Institute of Energy Technology Evaluation and Planning (KETEP) grant funded by the Korea government Ministry of Knowledge Economy (RS-2024-00439210).

REFERENCES

[1] G. Engel, “KATS experiments to simulate corium spreading in the EPR core catcher concept.” No. FZKA--6475. (2000).
[2] J. J. Sienicki and M. T. Farmer, “Spreading of molten corium in Mk I geometry following vessel meltthrough”. No. CONF-881011-34. Argonne National Lab, IL, USA (1988)
[3] W. Tromm, J. J. Foit, and D. Magallon. “Dry and wet spreading experiments with prototypic material at the FARO facility and theoretical analysis.” No. FZKA--6475. (2000).
[4] J. Christophe, "Ex-vessel corium spreading: results from the VULCANO spreading tests." Nuclear Engineering and Design. 223(1) pp. 75-102 (2003)
[5] J. Christophe, "The VULCANO VE-U7 Corium spreading benchmark." Progress in Nuclear Energy. 48(3) pp. 215-234 (2006)
[6] J. Christophe, “Two-dimensional interaction of oxidic corium with concretes: The VULCANO VB test series.” Annals of Nuclear Energy. 36(10), pp. 1597-1613 (2009)
[7] M. T. Farmer, “Melt spreading code assessment, modifications, and application to the EPR core catcher design. " Atomic Energy Society of Japan, No. ANL-09/10, Argonne, IL, United States, (2009)
[8] B. Spindler, and J. M. Veteau. "The simulation of melt spreading with THEMA code: part 1: model, assessment strategy and assessment against analytical and numerical solutions." Nuclear engineering and design. 236(4), pp. 415-424 (2006)
[9] B. Spindler, and J. M. Veteau. "The simulation of melt spreading with THEMA code: Part 2: Assessment against

spreading experiments." Nuclear engineering and design. 236(4) pp. 425-441 (2006)
[10] R. Wittmaack, "Corflow: a code for the numerical simulation of free-surface flow." Nuclear technology. 119(2), pp. 158-180 (1997)
[11] T. Kawahara, "Ex-vessel molten core solidification behavior by moving particle semi-implicit method." Journal of nuclear science and technology 49(12), pp. 1156-1164 (2012)
[12] H. Ikeda, "Numerical analysis of fragmentation processes of liquid metal in vapor explosions using moving particle semi-implicit method." Nippon Kikai Gakkai Ronbunshu. 64(624), pp 2431-2437. (1998)
[13] J. R. Shewchuk, "An introduction to the conjugate gradient method without the agonizing pain." (1994)
[14] S. J. Stedman, J. R. G. Evans, and J. Woodthorpe. "Rheology of composite ceramic injection moulding suspensions." Journal of materials science. 25(3), pp. 1833-1841. (1990).